Supplemental Table 1: Random Model Comparison in scTrio-seq2 data

| Model | Precision | Recall | F1 score | Accuracy |
|---|---|---|---|---|
| GE_PDI (Random) | 0.90 ± 0.0310 | 0.88 ± 0.0538 | 0.87 ± 0.0698 | 0.87 ± 0.0590 |
| GE_PDI | 0.93 ± 0.0113 | 0.92 ± 0.0104 | 0.92 ± 0.0105 | 0.92 ± 0.0096 |
| DM_PDI (Random) | 0.90 ± 0.0098 | 0.90 ± 0.0082 | 0.90 ± 0.0072 | 0.92 ± 0.0041 |
| DM_PDI | 0.93 ± 0.0087 | 0.92 ± 0.0098 | 0.92 ± 0.0095 | 0.93 ± 0.0075 |
| GE_PPI (Random) | 0.88 ± 0.0021 | 0.90 ± 0.0014 | 0.88 ± 0.0020 | 0.89 ± 0.0025 |
| GE_PPI | 0.89 ± 0.0658 | 0.89 ± 0.0600 | 0.88 ± 0.0792 | 0.88 ± 0.0647 |
| DM_PPI (Random) | 0.86 ± 0.0112 | 0.85 ± 0.0194 | 0.85 ± 0.0188 | 0.87 ± 0.0111 |
| DM_PPI | 0.91 ± 0.0059 | 0.91 ± 0.0089 | 0.91 ± 0.0079 | 0.92 ± 0.0074 |
| GE_DM_PDI (Random) | 0.92 ± 0.0073 | 0.91 ± 0.0082 | 0.91 ± 0.0087 | 0.91 ± 0.0082 |
| GE_DM_PDI | 0.91 ± 0.0134 | 0.91 ± 0.0096 | 0.90 ± 0.0124 | 0.90 ± 0.0120 |
| GE_DM_PPI (Random) | 0.77 ± 0.1819 | 0.79 ± 0.1586 | 0.76 ± 0.1872 | 0.82 ± 0.1186 |
| GE_DM_PPI | 0.92 ± 0.0240 | 0.91 ± 0.0316 | 0.91 ± 0.0319 | 0.92 ± 0.0267 |
| BioLM-NET (Random PDI,PPI connections) | 0.53 ± 0.1278 | 0.60 ± 0.0688 | 0.53 ± 0.0907 | 0.67 ± 0.0526 |
| BioLM-NET (Random PDI,PPI, pathway connections, LLM embedding) | 0.88 ± 0.0299 | 0.90 ± 0.0287 | 0.88 ± 0.0371 | 0.89 ± 0.0538 |

Supplemental Table 2: Significant GO terms from our top 50 SHAP ranked genes in the gene expression branch in ROSMAP data

| ID | Description |
|---|---|
| GO:0099519 | dense core granule cytoskeletal transport |
| GO:1901950 | dense core granule transport |
| GO:0008090 | retrograde axonal transport |
| GO:0032253 | dense core granule localization |
| GO:0032252 | secretory granule localization |
| GO:0047496 | vesicle transport along microtubule |
| GO:0008089 | anterograde axonal transport |
| GO:0098937 | anterograde dendritic transport |
| GO:1905383 | protein localization to presynapse |
| GO:0099518 | vesicle cytoskeletal trafficking |
| GO:0098935 | dendritic transport |
| GO:0098840 | protein transport along microtubule |
| GO:0099118 | microtubule-based protein transport |
| GO:0098930 | axonal transport |
| GO:0051145 | smooth muscle cell differentiation |
| GO:0008088 | axo-dendritic transport |

| | |
|---|---|
| GO:0032011 | ARF protein signal transduction |
| GO:0032012 | regulation of ARF protein signal transduction |
| GO:0072384 | organelle transport along microtubule |
| GO:0060004 | reflex |
| GO:0005871 | kinesin complex |
| GO:1904115 | axon cytoplasm |
| GO:0035253 | ciliary rootlet |
| GO:0120111 | neuron projection cytoplasm |
| GO:0099524 | postsynaptic cytosol |
| GO:0032839 | dendrite cytoplasm |
| GO:0099522 | cytosolic region |
| GO:0008574 | plus-end-directed microtubule motor activity |
| GO:0008017 | microtubule binding |
| GO:0003777 | microtubule motor activity |
| GO:0015631 | tubulin binding |
| GO:0003774 | cytoskeletal motor activity |

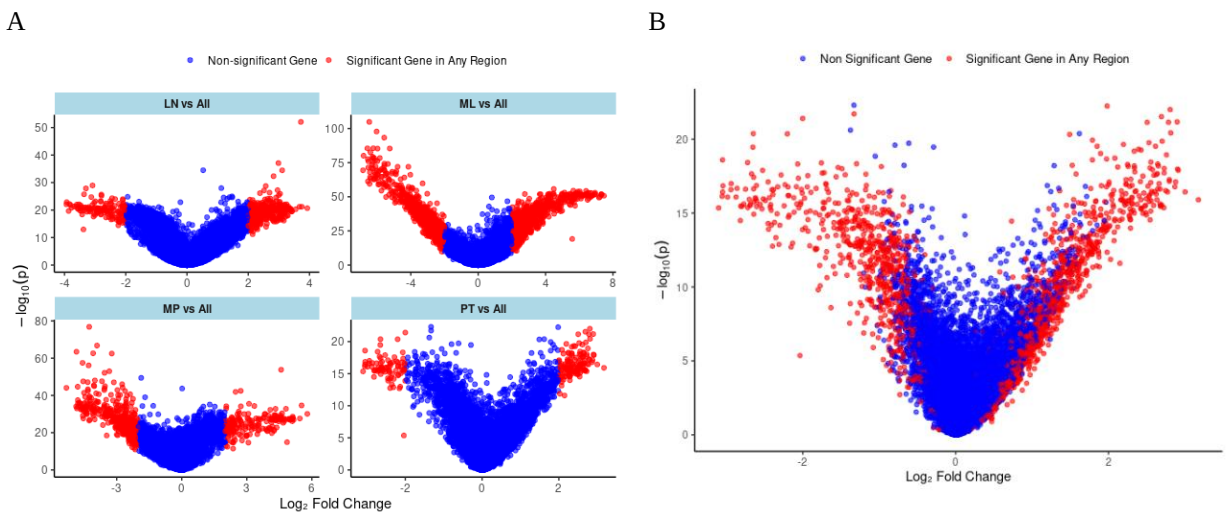


Supplemental Fig. 1. A. Volcano plot for DE analysis between LN vs All, ML vs All, MP vs All and PT vs All and B. volcano plot for final DE genes. In scTrio-seq2 data

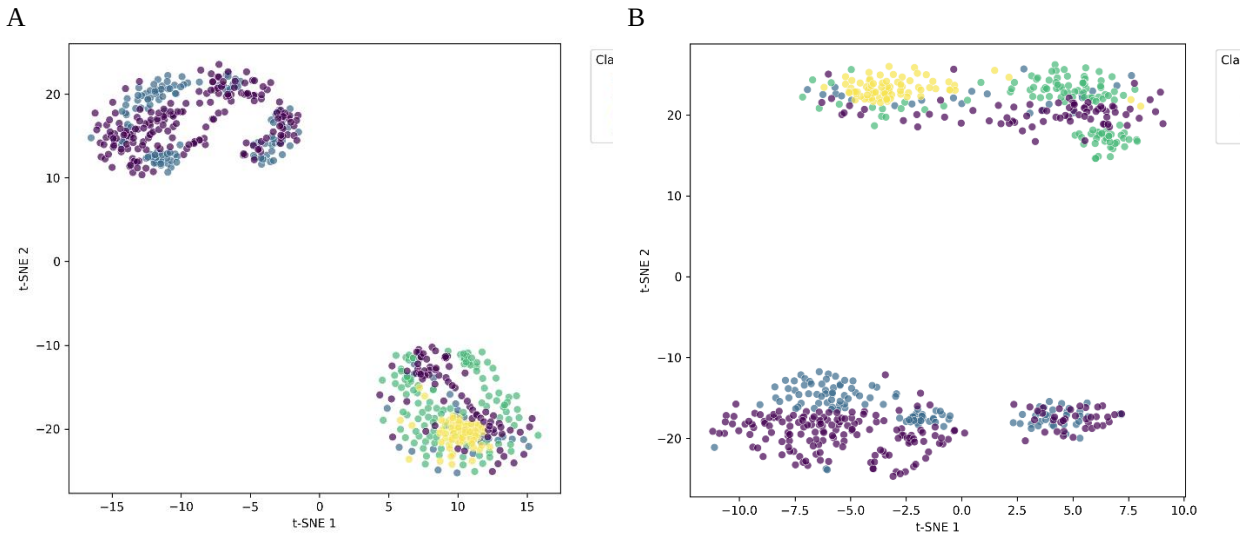


Supplemental Fig. 2. A. All gene t-SNE B. DE gene t-SNE in scTrio-seq2 data

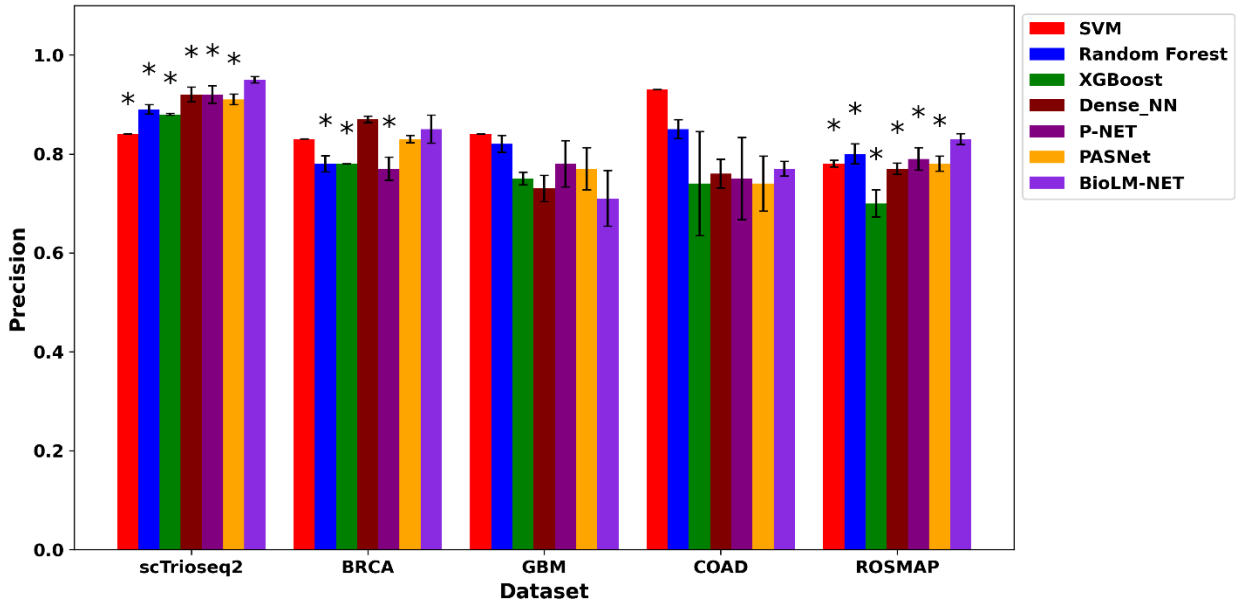


Supplemental Fig. 3. Precision comparison of BioLM-NET with baseline and SOTA models. Wilcoxon rank sum test was performed by comparing BioLM-NET with other models (p-value < 0.05 is denoted by *)

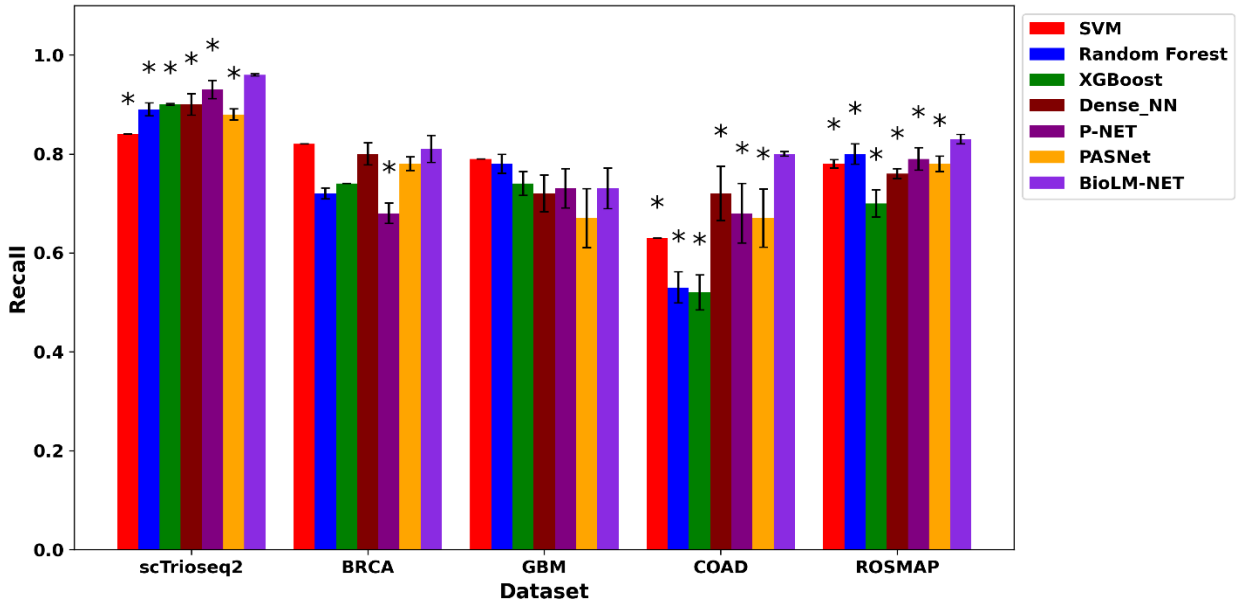


Supplemental Fig. 4. Recall comparison of BioLM-NET with baseline and SOTA models. Wilcoxon rank sum test was performed by comparing BioLM-NET with other models (p-value < 0.05 is denoted by *)

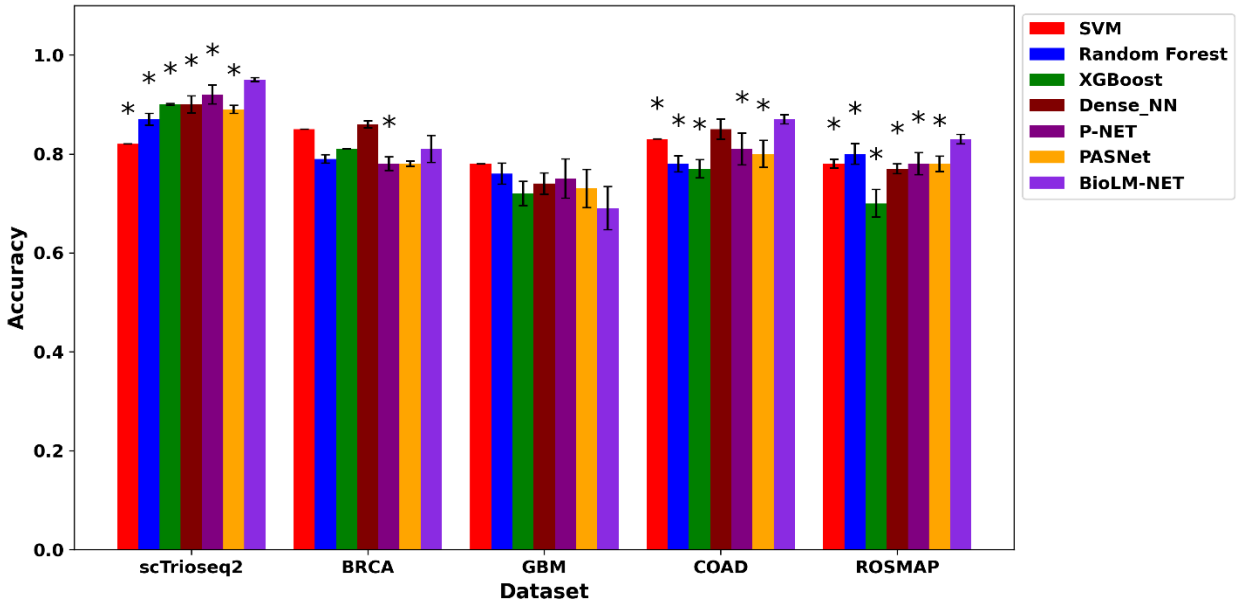


Supplemental Fig. 5. Accuracy comparison of BioLM-NET with baseline and SOTA models. Wilcoxon rank sum test was performed by comparing BioLM-NET with other models (p-value < 0.05 is denoted by *)

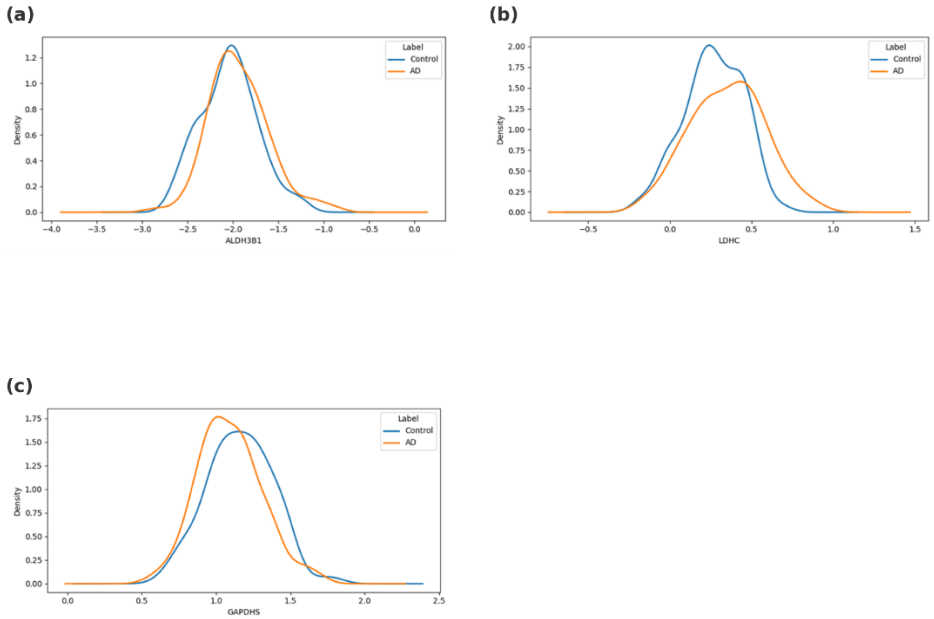


Supplemental Fig 6. DNA Methylation values (M-value) between Control vs AD patients in three genes that are derived from ROSMAP DNA Methylation SHAP ranked top 50 gene.

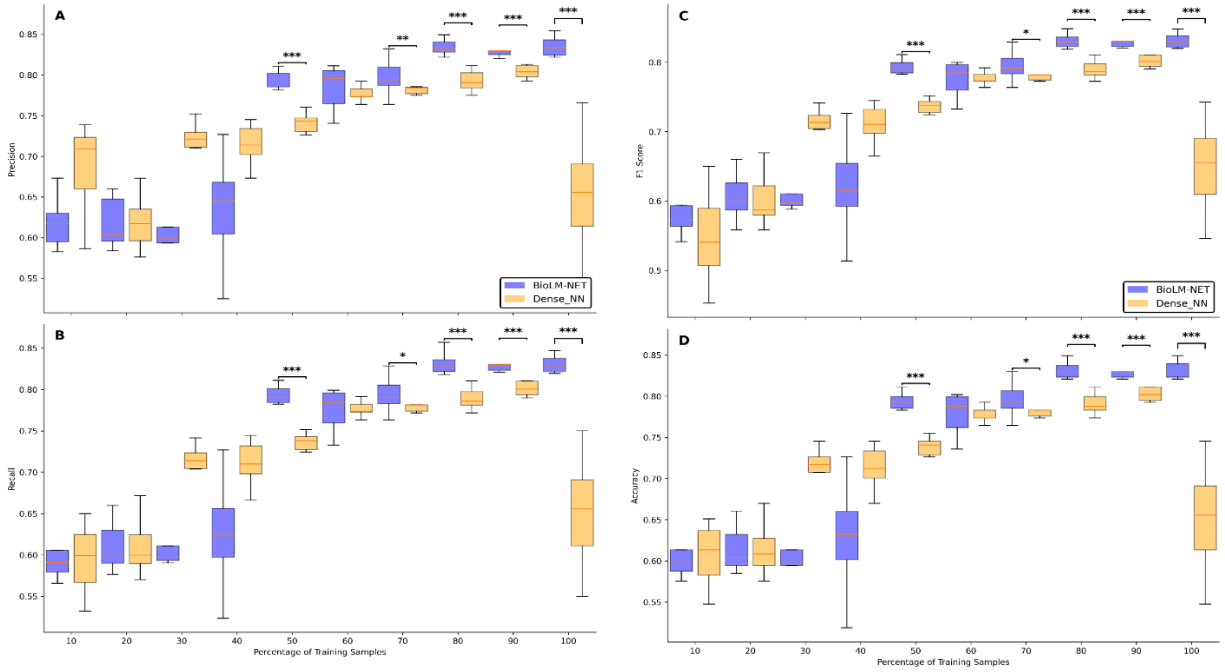


Supplemental Fig 7. Boxplots of (A)Precision (B) Recall (C) F1 score (D) Accuracy for BioLM-NET (blue) and Dense_NN (orange) across 10 independent runs at each percentage of training samples. Statistical significance was assessed with respect to BioLM-NETwith an one-sided Wilcoxon rank sum test (***: p-value < 0., **: p-value < 0.01, *: p-value < 0.05)

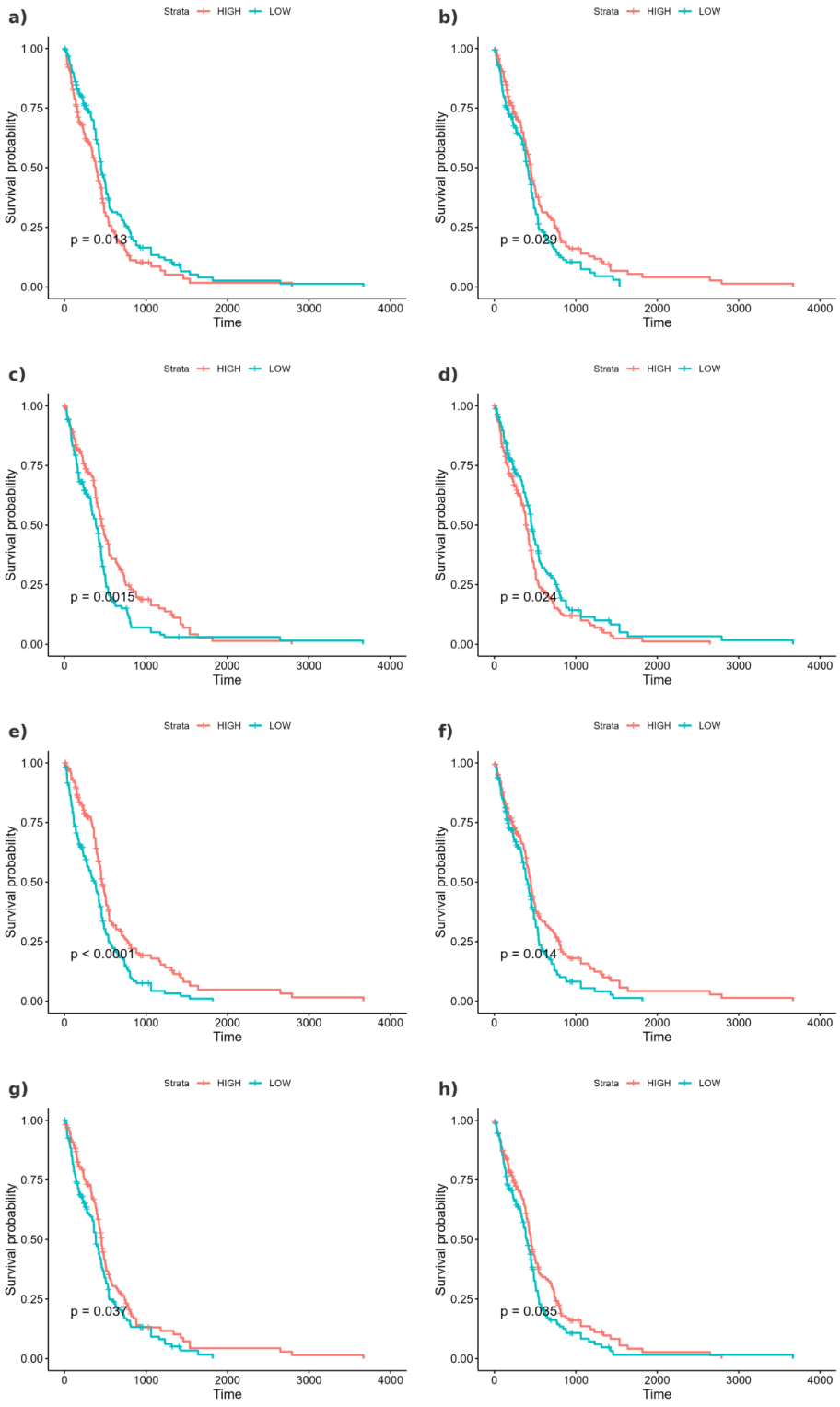


Supplemental Fig 8. Kaplan-Meier Plot for GBM (Gene expression features) : Kaplan–Meier survival curves for TCGA-GBM patients stratified by high vs. low expression of a. *CBX7*, *b. CENPJ*, *c. DACH1*, *d. NUDT22*, *e. PM20D2*, *f. RALGAPA1P1*, *g. TBX3*, *h. WDPCP*.

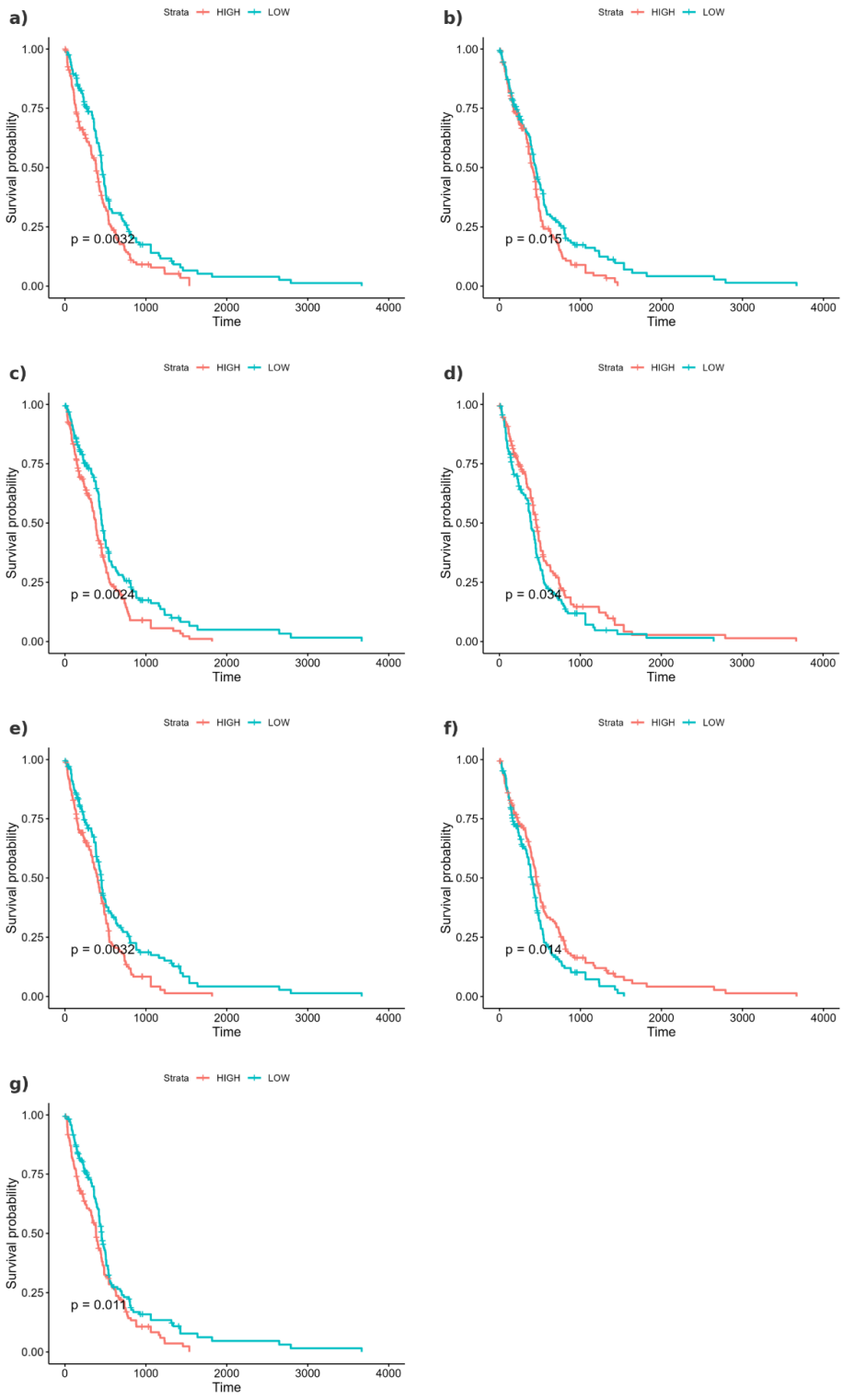


Supplemental Fig 9. Kaplan-Meier Plot for GBM (DNA Methylation features) patients stratified by high vs. low expression of (a) *C16orf89*, (b) *CANT1*, (c) *CDKN2D*, (d) *CPS1*, (e) *ELSPBP1*, (f) *GON4L*, and (g) *LDLRAP1*.

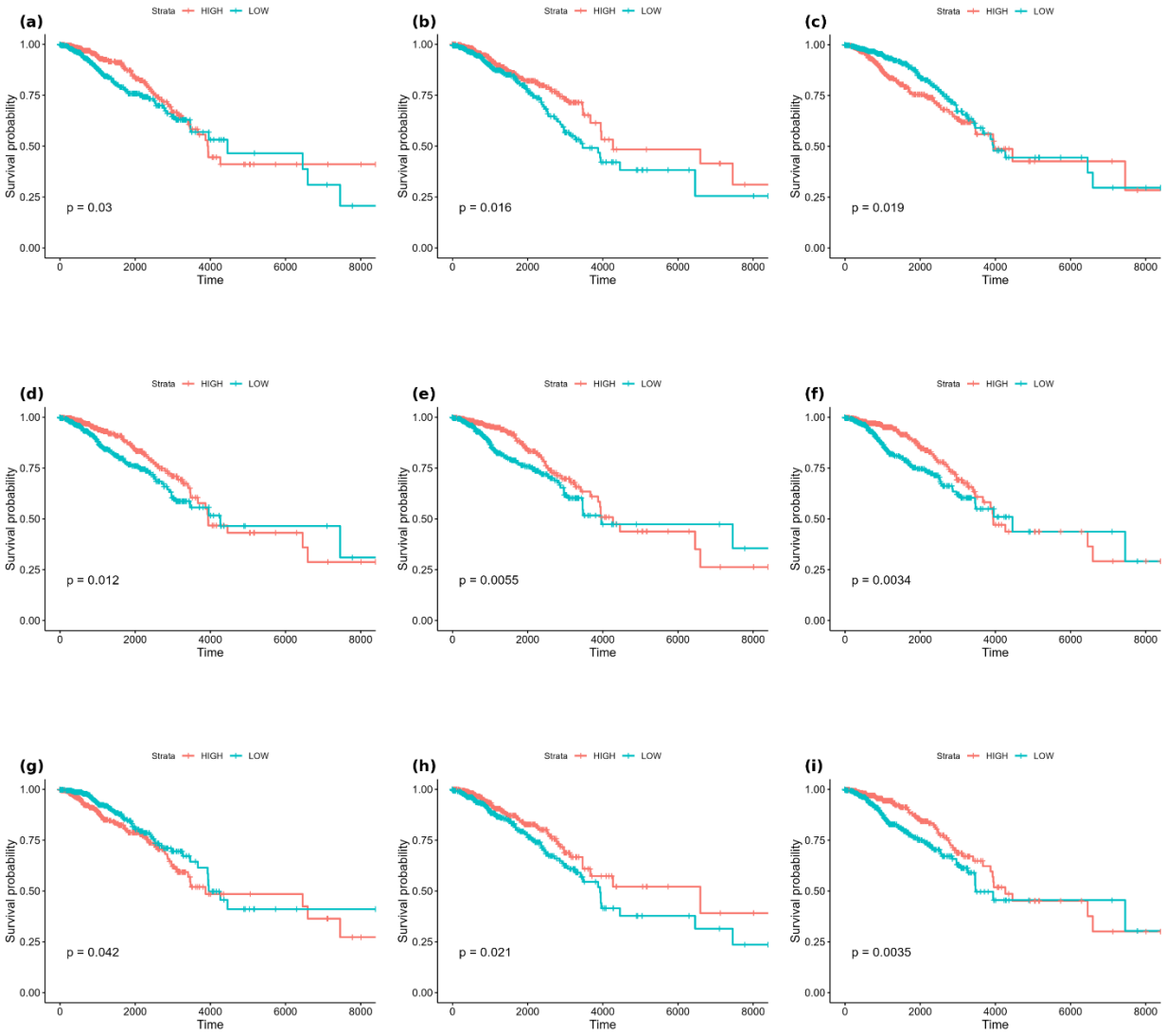


Supplemental Fig 10. Kaplan-Meier Plot for BRCA (Gene Expression features) patients stratified by high vs. low expression of (a) *BCL2*, (b) *CXCL1*, (c) *EIF2S2*, (d) *FGD3*, (e) *KDM4B*, (f) *NXNL2*, (g) *SOX11*, (h) *SPARCL1*, and (i) *SUSD3*.

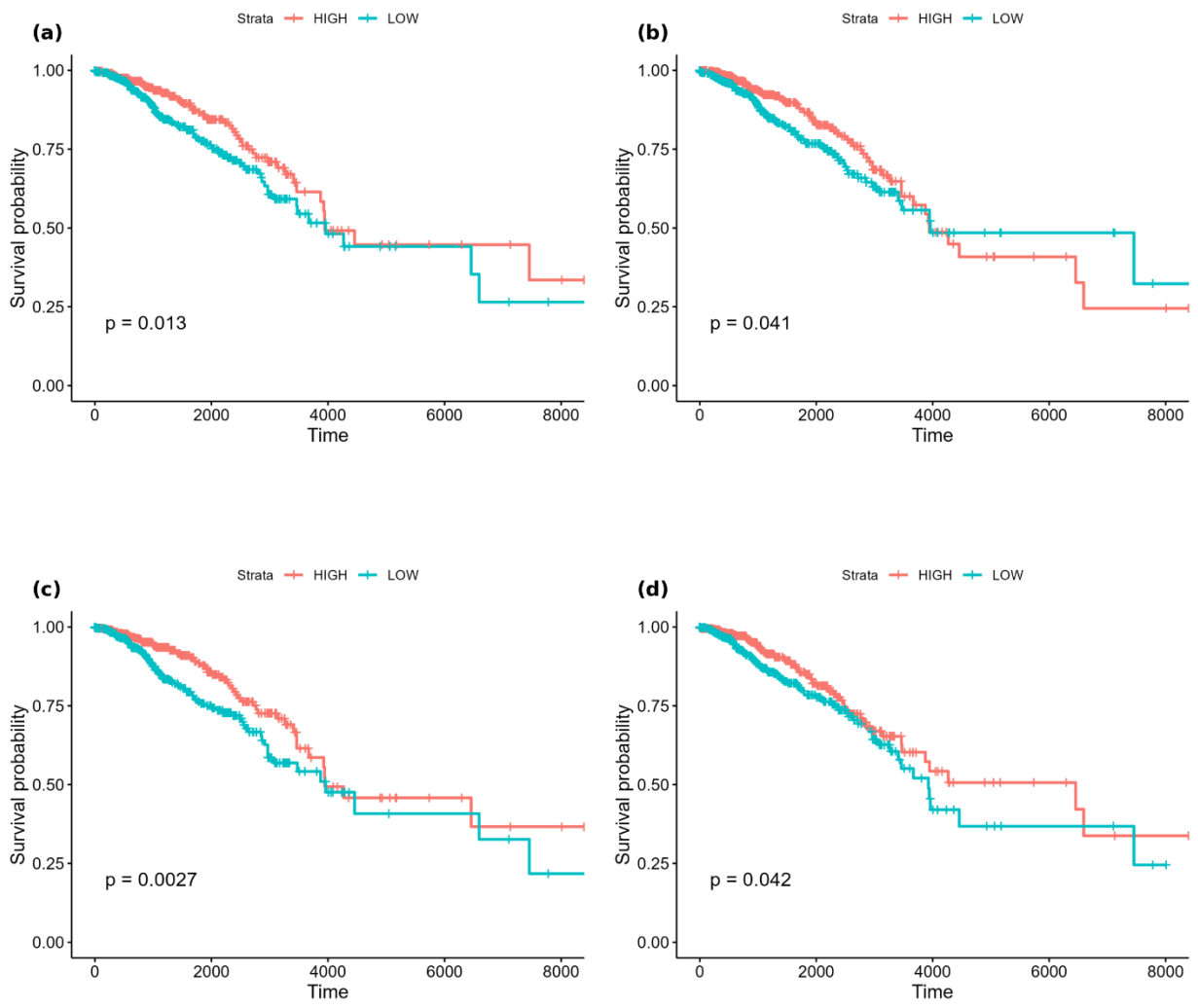


Supplemental Fig 11. Kaplan-Meier survival curves for BRCA (DNA Methylation features) patients stratified by high vs. low expression of (a) *IGFALS*, (b) *IGFBP4*, (c) *SCUBE2*, and (d) *SERPINA12*.

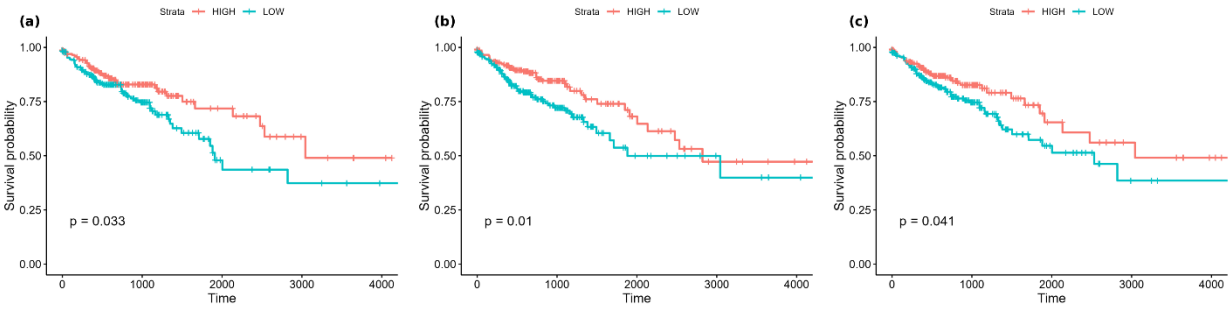


Supplemental Fig 12. Kaplan-Meier survival curves for COAD (Gene Expression features) patients stratified by high vs. low expression of (a) *ASPHD2* and (b) *COX11*.

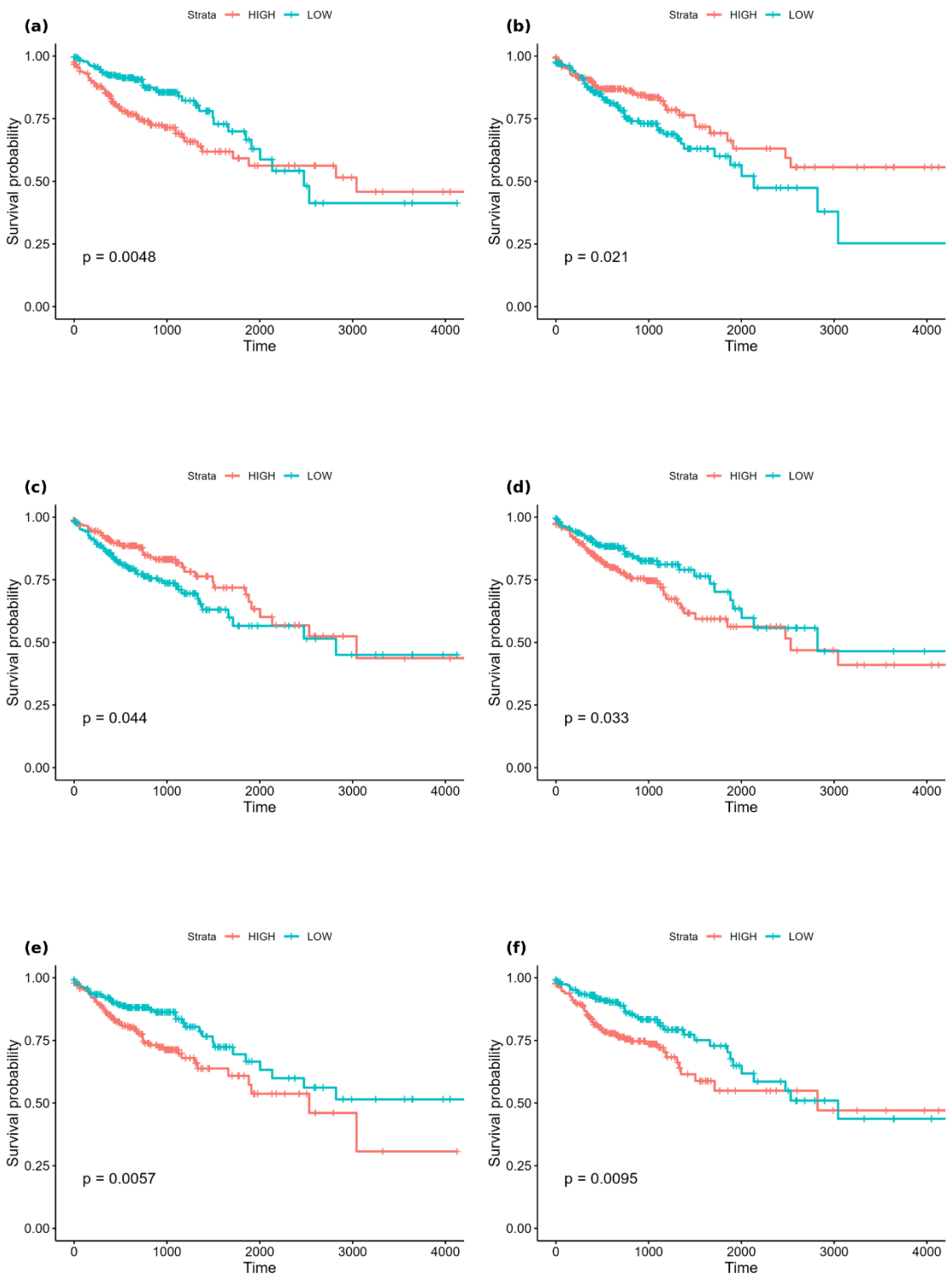


Supplemental Fig 13 . Kaplan-Meier survival curves for COAD (DNA Methylation features) patients stratified by high vs. low expression of (a) *ARRDC1*, (b) *CAMTA1* , (c) *CDC14A* , (d) *DNAJC17* , (e) *FABP4* , (f) *FGF22*

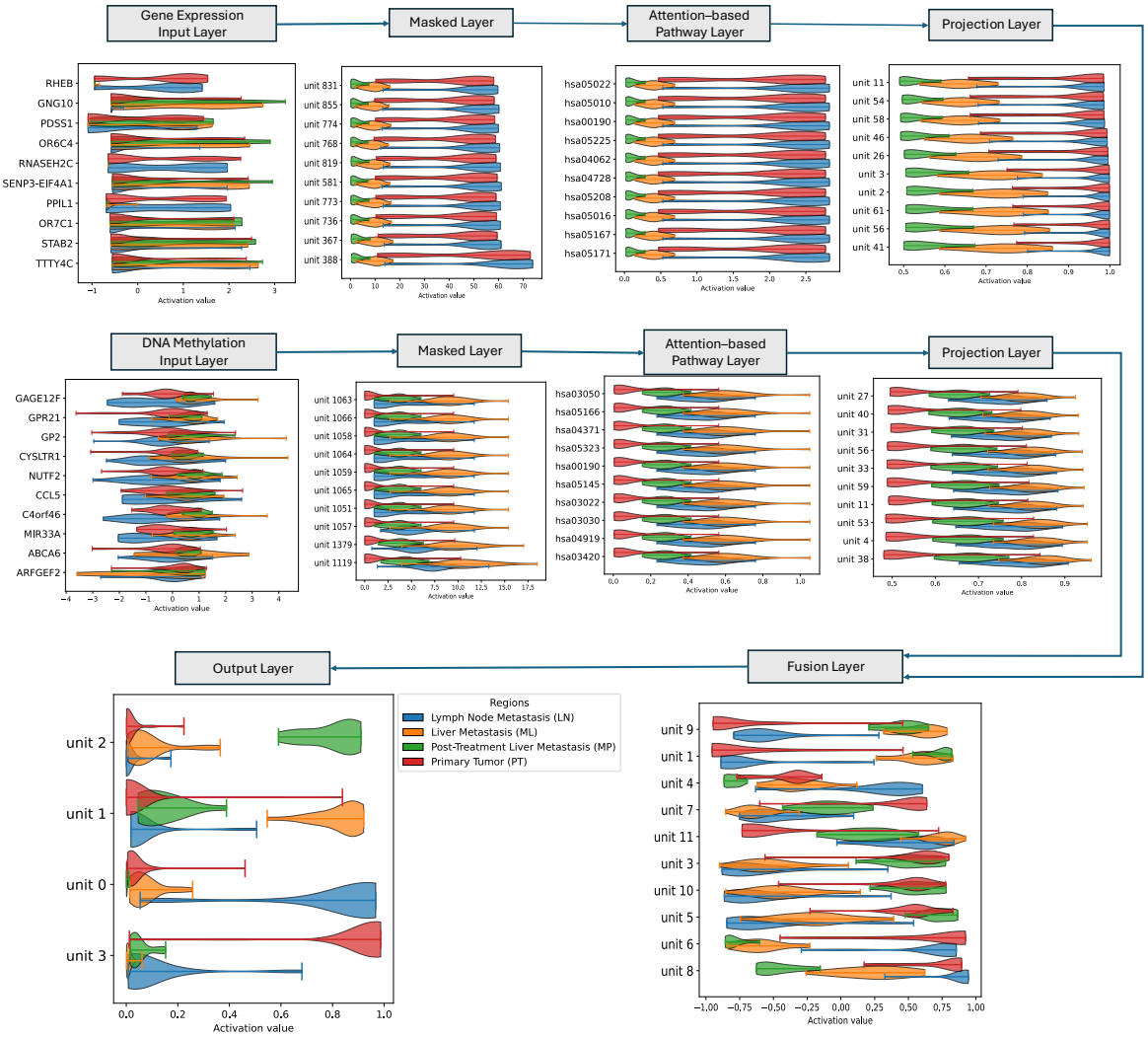


Supplemental Fig 14. Activation score of top 10 node from each layer. Output has 4 nodes.